Is the Structure of ^{42}Si Understood?

A. Gade,[1,2] B. A. Brown,[1,2] J. A. Tostevin,[3] D. Bazin,[1,2] P. C. Bender,[1,*] C. M. Campbell,[4] H. L. Crawford,[4] B. Elman,[1,2] K. W. Kemper,[5] B. Longfellow,[1,2] E. Lunderberg,[1,2] D. Rhodes,[1,2] and D. Weisshaar[1]

[1]*National Superconducting Cyclotron Laboratory, Michigan State University, East Lansing, Michigan 48824, USA*
[2]*Department of Physics and Astronomy, Michigan State University, East Lansing, Michigan 48824, USA*
[3]*Department of Physics, University of Surrey, Guildford, Surrey GU2 7XH, United Kingdom*
[4]*Nuclear Science Division, Lawrence Berkeley National Laboratory, California 94720, USA*
[5]*Department of Physics, Florida State University, Tallahassee, Florida 32306, USA*

(Received 12 March 2019; revised manuscript received 23 April 2019; published 4 June 2019)

A more detailed test of the implementation of nuclear forces that drive shell evolution in the pivotal nucleus ^{42}Si—going beyond earlier comparisons of excited-state energies—is important. The two leading shell-model effective interactions, SDPF-MU and SDPF-U-Si, both of which reproduce the low-lying $^{42}\mathrm{Si}(2_1^+)$ energy, but whose predictions for other observables differ significantly, are interrogated by the population of states in neutron-rich ^{42}Si with a one-proton removal reaction from ^{43}P projectiles at 81 MeV/nucleon. The measured cross sections to the individual ^{42}Si final states are compared to calculations that combine eikonal reaction dynamics with these shell-model nuclear structure overlaps. The differences in the two shell-model descriptions are examined and linked to predicted low-lying excited 0^+ states and shape coexistence. Based on the present data, which are in better agreement with the SDPF-MU calculations, the state observed at 2150(13) keV in ^{42}Si is proposed to be the (0_2^+) level.

DOI: 10.1103/PhysRevLett.122.222501

Modeling the nuclear landscape with predictive power, including the most exotic nuclei near the limits of nuclear existence, is an overarching goal driving 21st century nuclear science. This quest thrives through the interplay of experiment and theory, whereby observables measured for very neutron-proton asymmetric nuclei reveal isospin-dependent aspects of the nuclear force. They also identify benchmark nuclei, critical for understanding and for quantitative extrapolations toward the shortest-lived rare isotopes—many outside of the reach of laboratory studies but whose properties underpin the modeling of nucleosynthesis processes, for example. Over the few decades of rare-isotope research, certain nuclei defying textbook expectations have emerged as pivotal—they are typically located in regions of rapid structural change or at the extremes of weak binding where open quantum systems properties are exhibited. The $Z = 14$ isotope $^{42}\mathrm{Si}_{28}$ is one such nucleus.

At present, the most neutron-rich Si isotope known to exist is ^{44}Si, with neutron number $N = 30$ [1], and the most neutron-rich $N = 28$ isotone with known spectroscopic information is ^{40}Mg [2]. This places their even-even neighbor ^{42}Si ($Z = 14$, $N = 28$) at the frontier of nuclear experimentation. A description of ^{42}Si has challenged nuclear structure physics for a long time. Early on, the β-decay half-life of ^{42}Si [3] and the particle stability of ^{43}Si [4] were interpreted as indicators that the $N = 28$ magic number had broken down, but that a pronounced $Z = 14$ subshell closure may prevent ^{42}Si from being well deformed [5–8]. These speculations were resolved by the first successful spectroscopy of ^{42}Si [9], revealing a surprisingly low-lying first 2^+ state, at $E(2_1^+) = 770(19)$ keV, the onset of collectivity, and the breakdown of the $N = 28$ magic number in ^{42}Si.

Reproducing this evolution, (a) along the Si isotopic chain, starting from doubly magic $^{34}\mathrm{Si}_{20}$, with the rapid increase in collectivity or deformation at $N = 28$, and (b) along the isotone line from doubly magic $^{48}\mathrm{Ca}_{28}$ toward Si, has been a formidable challenge for the nuclear shell model. Two shell-model effective interactions, SDPF-U [10] and SDPF-MU [11], succeeded to reproduce a low-lying 2_1^+ state in ^{42}Si [12]. The mechanism underlying the collapse of the $N = 28$ shell gap was attributed to (i) the filling of the neutron $0f_{7/2}$ orbit reducing the $Z = 14$ gap relative to ^{34}Si, and, in concert, (ii) the removal of protons from the $0d_{3/2}$ orbit reducing the $N = 28$ gap relative to ^{48}Ca, both the result of the proton-neutron monopole parts of the tensor force [13]. $\Delta l, j = 2$ quadrupole correlations, reaching across the so-narrowed $Z = 14$ and $N = 28$ gaps, then mutually enhance one another leading to deformation, as argued within the context of an SU(3)-like scheme [9,10] or a nuclear Jahn-Teller effect [11]. While both shell-model interactions reproduce the low-energy first-excited $^{42}\mathrm{Si}(2^+)$ state, their predictions for the level density and energies of states beyond the first 2^+ differ dramatically. This demands confrontation with additional experimental data to validate

these different implementations of the suspected drivers of rapid shell evolution in this benchmark region [14–19], where the spectrum of the near-dripline nucleus ^{40}Mg turned out to be surprising [2].

It required half a decade and a new-generation accelerator facility for spectroscopy beyond the ^{42}Si first-excited state to be performed [20]. There, the ^{12}C(^{44}S, ^{42}Si $+\gamma$)X two-proton removal reaction was used to populate excited states in ^{42}Si. The first 4^+ state was suggested at 2173(14) keV, with the ratio $R_{4/2} = E(4_1^+)/E(2_1^+)$ close to the rotational limit, as one may expect for a well-deformed nucleus [20]. However, a direct reaction model analysis, using the SDPF-U/SDPF-U-Si and SDPF-MU shell-model two-nucleon amplitudes [21], could not reconcile the γ-ray spectra and assignments reported in Ref. [20], indicating that ^{42}Si was not understood within the current shell-model picture after all; one-proton removal to ^{42}Si was proposed to clarify the situation [21].

Here, we report this first high-resolution in-beam γ-ray spectroscopy of ^{42}Si in the direct one-proton removal reaction ^{9}Be(^{43}P, ^{42}Si $+\gamma$) using GRETINA [22,23]. The measured partial removal cross sections are compared to direct reaction calculations combining eikonal dynamics and shell-model spectroscopic factors. We probe the different implementations of the drivers of shell evolution on the valence single-particle levels through the theoretical spectroscopic factors from the SDPF-MU and SDPF-U-Si shell-model calculations. The stark differences in observables (other than the 2_1^+ energy) predicted by the two shell-model descriptions of ^{42}Si reveal that this key nucleus is not yet sufficiently understood.

The secondary beam of ^{43}P was produced by fragmentation of a 140 MeV/nucleon stable ^{48}Ca beam, delivered by the Coupled Cyclotron Facility at NSCL [24], impinging on a 1363 mg/cm^2 ^{9}Be production target and separated using a 150 mg/cm^{2}Al degrader in the A1900 fragment separator [25]. The momentum acceptance of the separator was set to transmit $\Delta p/p = 3\%$, yielding rates of typically 45 ^{43}P/s. About 20% of the secondary beam composition was ^{43}P, with ^{42}P and ^{44}S as the most intense other components.

The secondary ^{9}Be reaction target (476 mg/cm^2 thick) was located at the target position of the S800 spectrograph. Reaction products were identified on an event-by-event basis in the S800 focal plane with the standard focal-plane detector systems [26]. The inclusive cross section for the one-proton knockout from ^{43}P to ^{42}Si was measured to be $\sigma_{\rm inc} = 3.4(2)$ mb.

The γ-ray detection system GRETINA [22,23], an array of 40 high-purity Ge crystals that are each 36-fold segmented, was used to detect the prompt γ rays emitted by the reaction residues. The 10 detector modules—with four crystals each—were arranged in two rings, with four modules located at 58° and six at 90° with respect to the beam axis. Online signal decomposition provided γ-ray interaction points (xyz) for event-by-event Doppler reconstruction of the photons emitted in-flight at $v/c \approx 0.4$. The information on the momentum vector of projectilelike reaction residues, as reconstructed through the spectrograph, was incorporated into the Doppler correction. Figure 1 shows the Doppler-reconstructed γ-ray spectrum for ^{42}Si with nearest-neighbor addback included [23]. It is apparent that only little cross section is carried by excited states beyond the 2_1^+ level. Nevertheless, the remarkable peak-to-background ratio allows for spectroscopy at such modest levels of statistics and, as shown in the inset of Fig. 1, weak peak structures at 1413(10), 2037(10), 2351(10), and 2743(10) keV are visible, in addition to the strong $2_1^+ \rightarrow 0_1^+$ transition at 737(8) keV. The lowest three of these higher-energy γ rays likely correspond to the 1431(11), 2032(9), and 2357(15) keV transitions reported in Ref. [20].

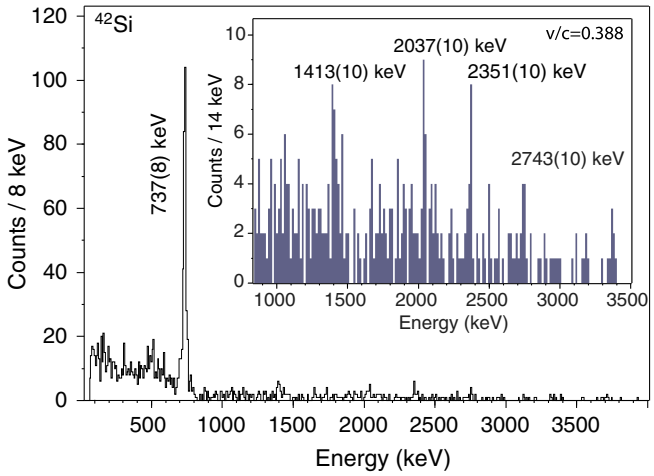

FIG. 1. Gamma-ray spectrum in coincidence with ^{42}Si reaction residues, event-by-event Doppler reconstructed and including nearest-neighbor addback. The inset shows the high-energy region expanded.

In spite of the low statistics at high excitation energy, a coincidence analysis provides some limited guidance for the placement of the transitions in the level scheme. Figure 2(a) shows the projection of the $\gamma\gamma$ coincidence matrix and the coincidences with the $2_1^+ \rightarrow 0_1^+$ transition (inset). In comparison to the γ-ray singles spectrum of Fig. 1, the projection of the coincidence matrix shows a significantly increased number of counts at $E > 800$ keV relative to the 737-keV peak counts, indicating that the high-energy region bears coincidences. Because of the low statistics, no peaks are expected in the coincidence spectrum (inset) but groups of counts appear to cluster where, with more statistics, the peaks and/or Compton edges of the transitions reported here would occur. Turning the analysis around and showing the sum of cut spectra coincident with the 1.4, 2.0, 2.3, and 2.7 MeV photopeaks returns the $2_1^+ \rightarrow 0_1^+$ transition at about the right intensity for all

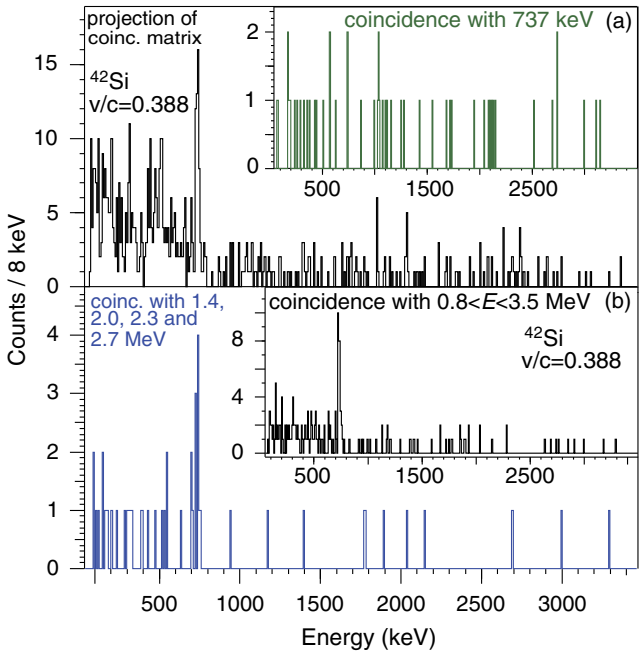

FIG. 2. (a) Projection of the $\gamma\gamma$ coincidence matrix and coincidences with 737 keV (inset). (b) Summed coincidence spectrum obtained from gates on the photopeaks of all higher-energy γ-ray transitions and coincidences with $0.8 < E < 3.5$ MeV (inset). Spectra are not background subtracted.

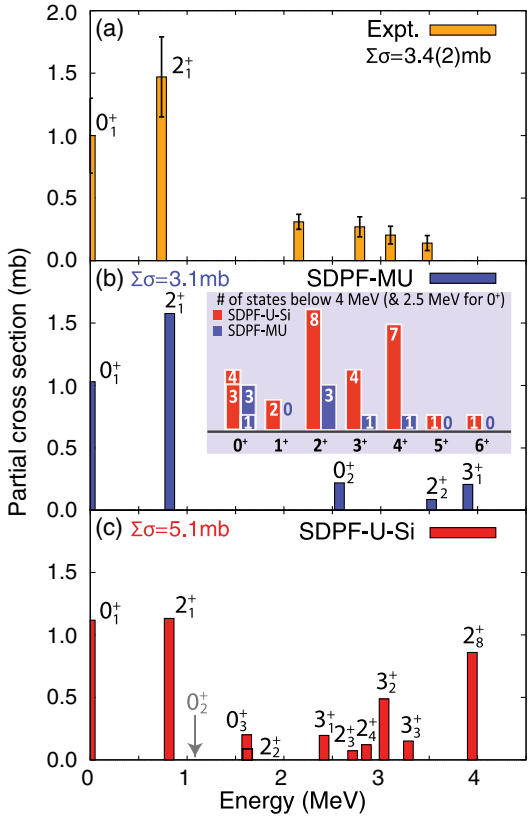

FIG. 3. Partial proton removal cross sections from ^{43}P to bound states in ^{42}Si: (a) experiment, (b) direct reaction theory with SDPF-MU shell-model spectroscopic factors, and (c) direct reaction theory with SDPF-U-Si shell-model spectroscopic factors. For the calculations, states up to 4 MeV and carrying $C^2S > 0.02$ spectroscopic strengths were included and $R_s = 0.3$ was applied. The inset to (b) shows, for each of the effective interactions, the number of states below 4 MeV (and additionally below 2.5 MeV for the 0^+ states).

higher-lying transitions to be coincident with it. The inset shows a coincident spectrum to the broad energy region of $0.8 < E < 3.5$, now including, in addition to the photopeaks, also the Compton continua. The number of counts in the $2_1^+ \rightarrow 0_1^+$ is increased by a factor of about 3 as one would expect from the peak-to-Compton ratio of GRETINA at these energies. We, therefore, tentatively propose that all of the higher-lying transitions reported here feed the first 2^+ state. All the resulting excited states lie below the (rather uncertain) neutron separation energy of $S_n = 3721(747)$ keV.

The photopeak efficiency of GRETINA was calibrated with standard sources and corrected for the Lorentz boost of the γ-ray distribution emitted by the residual nuclei moving at almost 40% of the speed of light and addback factors from GEANT simulations [27]. Partial cross sections to the specific final states were determined from the efficiency-corrected γ-ray peak areas, with discrete feeding subtracted, relative to the number of incoming ^{43}P projectiles and the number density of the target.

One-nucleon removal is a direct reaction with sensitivity to single-particle degrees of freedom. The cross sections for the population of individual states in the reaction residue depend sensitively on the overlap, and spectroscopic factor, of the projectile initial and the residue final states [28]. The shape of the ground-state residue parallel momentum distribution in the one-proton removal from ^{44}S to ^{43}P unambiguously revealed the knockout of an $s_{1/2}$ proton, determining the ground-state spin of ^{43}P to $1/2^+$ [29], in agreement with shell model.

Using the one-nucleon removal reaction methodology of Ref. [30] and shell-model spectroscopic factors, the partial cross sections to all bound, shell-model ^{42}Si final states were calculated. These are confronted with experiment in Fig. 3. A reduction factor $R_s = 0.3$, appropriate for the effective proton-neutron separation energy asymmetry from ^{43}P, $\Delta S \approx 16$ MeV [31,32], is applied to the calculated cross sections. The R_s and ΔS deduced from the measured and calculated cross sections (using SDPF-MU) are 0.33(2) and 15.6 MeV.

The measured cross-section distribution reflects the rather simple γ-ray spectrum, dominated by the $2_1^+ \rightarrow 0_1^+$ transition, with weak higher-energy transitions. The majority of the cross section feeds the ground state and the 2_1^+ level, with modest spectroscopic strength distributed between 2 and 3.5 MeV. The partial cross sections calculated with the SDPF-MU spectroscopic factors describe the measured cross-section distribution well, including the values of

σ_{inc}, $\sigma(0_1^+)$ and $\sigma(2_1^+)$ on the absolute scale and the fraction of the strength at higher excitation energy. Use of the SDPF-U-Si wave functions predicts a larger inclusive cross section and significantly more strength above 1.5 MeV, in particular, if the predicted 2_8^+ state at 3.945 MeV were bound. The cross-section distribution based on the SDPF-MU spectroscopy also better matches the measured distribution on a detailed level. The states predicted to be populated strongly are calculated to decay predominantly to the first 2^+ state, consistent with our proposed level scheme. The larger strength at higher excitation energy, predicted using SDPF-U-Si, is not supported by the γ-ray spectrum (see Fig. 1). For example, the 3_2^+ state at 3.034 MeV, predicted to carry significant strength, would decay with a $> 90\%$ branch to the 3_1^+ state with a $\sim$600 keV γ-ray transition that should be visible in the data with $\sim$60 peak counts. Similarly, if the 2_8^+ state were bound, the measured inclusive cross section should have been 30% higher and a γ-ray transition of order five times stronger than the 2.7 MeV peak should have been observed near 3.2 MeV. We conclude that the SDPF-MU interaction provides calculations in better agreement with the data than SDPF-U-Si.

This outcome seems rooted in the vastly different ^{42}Si level densities predicted using SDPF-U-Si and SDPF-MU. The insert to Fig. 3(b) illustrates this point through the number of states per J^+ value below 4 MeV (and also below 2.5 MeV for 0^+ states). SDPF-U-Si offers five more 2^+ and three more 3^+ states in this energy window, some of them predicted to carry substantial spectroscopic strengths and thus proton-removal cross section.

Perhaps the most remarkable difference is the number of low-lying 0^+ states generated by the two shell-model interactions, namely 4(3) and 3(1) below 4(2.5) MeV (including the ground state), from SDPF-U-Si and SDPF-MU, respectively. In fact, this abundance of low-lying 0^+ states in the SDPF-U-Si calculation appears to drive the high density of low-lying ^{42}Si levels, as compared to SDPF-MU. This is illustrated in Fig. 4 where, for the first 10 calculated states for each J^+ quantum number, the predicted $B(E2)$ electric quadrupole transition strengths to all other levels are indicated by lines. Here the line thickness scales with the $B(E2)$ values. Both calculations show a pronounced yrast line, formed by the strong intraband $E2$ decays between the first states of each even-J spin. For SDPF-MU, the 0_2^+ to 0_4^+ states are located beyond 2.5 MeV in excitation energy and are weakly connected with $E2$ transitions to the higher-lying 2^+ states that occur with significant level density above 3–4 MeV. The (isomeric) excited 0_2^+ state within SDPF-U-Si, however, appears to be the band head of an even-J band that carries collectivity comparable to the yrast band, as indicated by the similar $B(E2)$ values. The third and fourth 0^+ states are then predicted to be strongly connected to higher-lying 2^+ states which appear with significant level density starting at 2.5 MeV. The level structure from SDPF-U-Si is more compressed than that from the SDPF-MU calculation, leading to the markedly increased level density at low energies. The low-lying 0^+ states within SDPF-U-Si seem to play a role in this, with the second 0^+ state and the band structure built on top, constituting a remarkable case of predicted shape or configuration coexistence with essentially no connecting $E2$ transitions to the yrast band. Figure 4 also shows the neutron particle-hole content of the three lowest-lying 0^+ states relative to the closed-shell configuration [33]. Clearly, the wave functions of the 0^+ states differ significantly between the two calculations. Identifying and characterizing the excited 0^+ states and structures built on top of these will be a challenge for future experiments.

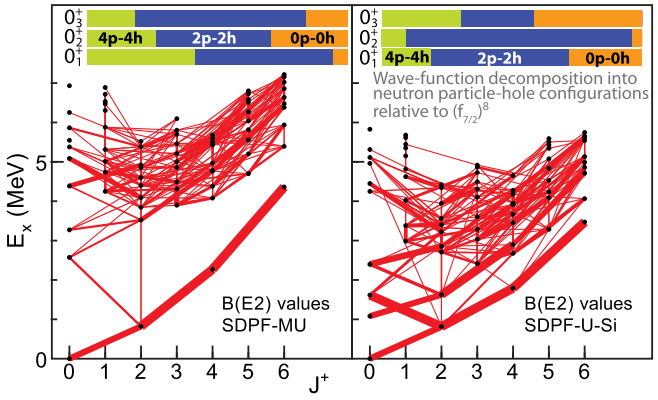

FIG. 4. Wave-function decomposition of the first three 0^+ states and network of $E2$ transitions as predicted by the SDPF-MU (left) and SDPF-U-Si (right) shell-model calculations. The first 10 states of each J^+ are computed together with their $B(E2)$ strength connecting to all other calculated states (displayed as connecting lines). The line thicknesses represent the $B(E2)$ strength of each transition.

Since ^{43}P has a $1/2^+$ ground state, only positive-parity states up to and including $J^\pi = 3^+$ can be populated directly by the removal of an sd-shell proton (see also Fig. 3). So, if the 1413 keV γ ray observed in this Letter corresponds to that reported in Ref. [20], the tentative (4_1^+) assignment made there for the corresponding state is thus not tenable. In the SDPF-MU picture, which is largely consistent with the present measurements, the possibility that the 1413-keV transition is due to indirect feeding is rather unlikely, since the populated 2_2^+ and 3_1^+ states are predicted to have only minuscule decay branches, of around 0.6% and 2%, respectively, to the 4_1^+. From Fig. 3 it seems, rather, that the state at 2150(13) keV may indeed be the first-exited 0^+ state, consistent also with its cross section and excitation energy predicted by SDPF-MU calculations. We note that the assignment of 0_2^+ for the 2150(13) keV level was also most consistent with the (SDPF-MU) two-proton removal cross-section analysis presented in Ref. [21]. One-proton removal data from ^{43}P with sufficient statistics to examine the shape of the

parallel momentum distribution of ^{42}Si in coincidence with the 1.4 MeV γ-ray transition would allow confirmation of this assignment if an $\ell = 0$ shape was found. At least an order of magnitude more statistics would be needed. A similar analysis is also possible for two-proton removal [21]. This challenge may have to await future, high-statistics experiments at a new-generation facility.

In summary, high-resolution in-beam γ-ray spectroscopy with GRETINA was performed for the neutron-rich nucleus ^{42}Si in a one-proton removal reaction from ^{43}P projectiles. Five γ-ray transitions are reported, four of which have been observed previously. Coincidence data were used to propose a tentative level scheme, which was then utilized to extract a partial-cross-section distribution for the direct one-proton removal reaction. The measured partial cross sections are confronted with direct reaction calculations that combine eikonal reaction dynamics with SDPF-MU and SDPF-U-Si shell-model spectroscopic information. These two effective interactions predict markedly different low-lying level densities with the scenario painted by the SDPF-MU calculations more consistent with the new data. This underscores the difficulty in extrapolating configuration-interaction calculations toward the neutron dripline and shows that nuclear models must be tested beyond the energy of the lowest 2^+ states. Our results highlight the SDPF-MU interaction as a starting point for understanding the role of weak binding for the isotone ^{40}Mg, for which both shell-model effective interactions fail to describe the observed, rather compressed, spectrum and where continuum effects are suggested to be at play [2]. From the selectivity of the reaction mechanism, and in agreement with similar theoretical work on the two-proton removal reaction leading to ^{42}Si, a level at 2150(13) keV is proposed to be the (0_2^+) state rather than the previously suggested (4_1^+) level. The differences in calculations from the two shell-model effective interactions are discussed and the special role of the low-lying 0^+ states is characterized. More final-state-exclusive experimental data are needed to further interrogate ^{42}Si and to clarify its description within the nuclear shell model. Ultimately, *ab-initio*–based Hamiltonians that incorporate the effects of the continuum are needed.

This work was supported by the U.S. National Science Foundation under cooperative Agreement No. PHY-1565546 and Grant No. PHY-1811855, by the U.S. Department of Energy (DOE) National Nuclear Security Administration through the Nuclear Science and Security Consortium under Award No. DE-NA0003180, and by the DOE-SC Office of Nuclear Physics under Grants No. DE-FG02-08ER41556 (NSCL) and No. DE-AC02-05CH11231 (LBNL). GRETINA was funded by the DOE, Office of Science. Operation of the array at N. S. C. L. was supported by the DOE under Grants No. DE-SC0014537 (NSCL) and No. DE-AC02-05CH11231 (LBNL). J. A. T. acknowledges support from the Science and Technology Facilities Council (UK) Grant No. ST/L005743/1. Discussions with Alfredo Poves are acknowledged.

*Present address: Department of Physics, University of Massachusetts Lowell, Lowell, Massachusetts 01854, USA.

[1] O. B. Tarasov, T. Baumann, A. M. Amthor, D. Bazin, C. M. Folden III, A. Gade, T. N. Ginter, M. Hausmann, M. Matos, D. J. Morrissey, A. Nettleton, M. Portillo, A. Schiller, B. M. Sherrill, A. Stolz, and M. Thoennessen, Phys. Rev. C **75**, 064613 (2007).
[2] H. L. Crawford, P. Fallon, A. O. Macchiavelli, P. Doornenbal, N. Aoi *et al.*, Phys. Rev. Lett. **122**, 052501 (2019).
[3] S. Grévy, J. C. Angèlique, P. Baumann, C. Borcea, A. Buta *et al.*, Phys. Lett. B **594**, 252 (2004).
[4] M. Notani, H. Sakurai, N. Aoi, Y. Yanagisawa, A. Saito *et al.*, Phys. Lett. B **542**, 49 (2002).
[5] P. D. Cottle and K. W. Kemper, Phys. Rev. C **58**, 3761 (1998).
[6] P. D. Cottle and K. W. Kemper, Phys. Rev. C **66**, 061301(R) (2002).
[7] J. Fridmann *et al.*, Nature (London) **435**, 922 (2005).
[8] J. Fridmann *et al.*, Phys. Rev. C **74**, 034313 (2006).
[9] B. Bastin, S. Grévy, D. Sohler, O. Sorlin, Zs. Dombradi *et al.*, Phys. Rev. Lett. **99**, 022503 (2007).
[10] F. Nowacki and A. Poves, Phys. Rev. C **79**, 014310 (2009).
[11] Y. Utsuno, T. Otsuka, B. A. Brown, M. Honma, T. Mizusaki, and N. Shimizu, Phys. Rev. C **86**, 051301(R) (2012).
[12] The effective interaction SDPF-U is formulated in two parts, one to be used for $Z \geq 15$ and one valid for $Z \leq 14$, called here SDPF-U-Si. This was taken into account for the overlaps used in this work.
[13] T. Otsuka, Phys. Scr. **T152**, 014007 (2013).
[14] R. Rodríguez-Guzmán, J. L. Egido, and L. M. Robledo, Phys. Rev. C **65**, 024304 (2002).
[15] L. Gaudefroy, Phys. Rev. C **81**, 064329 (2010).
[16] O. Sorlin, Phys. Scr. **T152**, 014003 (2013).
[17] E. Caurier, F. Nowacki, and A. Poves, Phys. Rev. C **90**, 014302 (2014).
[18] A. Gade and S. N. Liddick, J. Phys. G **43**, 024001 (2016).
[19] T. Otsuka, A. Gade, O. Sorlin, T. Suzuki, and Y. Utsuno, arXiv:1805.06501.
[20] S. Takeuchi, M. Matsushita, N. Aoi, P. Doornenbal, K. Li *et al.*, Phys. Rev. Lett. **109**, 182501 (2012).
[21] J. A. Tostevin, B. A. Brown, and E. C. Simpson, Phys. Rev. C **87**, 027601 (2013).
[22] S. Paschalis, I. Y. Lee, A. O. Macchiavelli, C. M. Campbell, M. Cromaz *et al.*, Nucl. Instrum. Methods Phys. Res., Sect. A **709**, 44 (2013).
[23] D. Weisshaar, D. Bazin, P. C. Bender, C. M. Campbell, F. Recchia *et al.*, Nuclear Instrum. Methods Phys. Res. A **847**, 187 (2017).
[24] A. Gade and B. M. Sherrill, Phys. Scr. **91**, 053003 (2016).
[25] D. J. Morrissey, B. M. Sherrill, M. Steiner, A. Stolz, and I. Wiedenhöver, Nucl. Instrum. Methods Phys. Res., Sect. B **204**, 90 (2003).
[26] D. Bazin, J. A. Caggiano, B. M. Sherrill, J. Yurkon, and A. Zeller, Nucl. Instrum. Methods Phys. Res., Sect. B **204**, 629 (2003).

[27] L. A. Riley (UCGretina GEANT4), Ursinus College (unpublished).
[28] J. A. Tostevin, J. Phys. G **25**, 735 (1999); P. G. Hansen and J. A. Tostevin, Annu. Rev. Nucl. Part. Sci. **53**, 219 (2003).
[29] L. A. Riley *et al.*, Phys. Rev. C **78**, 011303(R) (2008).
[30] A. Gade, P. Adrich, D. Bazin, M. D. Bowen, B. A. Brown, C. M. Campbell, J. M. Cook, T. Glasmacher, P. G. Hansen, K. Hosier, S. McDaniel, D. McGlinchery, A. Obertelli, K. Siwek, L. A. Riley, J. A. Tostevin, and D. Weisshaar, Phys. Rev. C **77**, 044306 (2008).
[31] J. A. Tostevin and A. Gade, Phys. Rev. C **90**, 057602 (2014).
[32] M. Wang, G. Audi, F. G. Kondev, W. J. Huang, S. Naimi, and Xing Xu, Chin. Phys. C **41**, 030003 (2017).
[33] In this presentation, 2p-2h contains about 10% of 1p-1h and 3p-3h content.